

Medium controlled aggregative growth as a key step in mesoporous silica nanoparticle formation

Viktoriya Semeykina* and Ilya Zharov*

Department of Chemistry, University of Utah, Salt Lake City, UT 84112

ABSTRACT: Near monodisperse mesoporous silica nanoparticles (MSN) represent a promising and rapidly developing type of mesoporous silica materials; however, the vast data on their synthesis remains unorganized and ill-understood. We systematically studied the formation of MSN under basic and neutral conditions using various temperatures, CTAB concentrations, hydrolyzing agents (triethanolamine, ammonia, phosphate buffers), and media with different colloidal stabilization properties (with ethanol as a cosolvent and monovalent salts). In the typical conditions for the preparation of stable MSN colloids, the particle size was controlled by colloidal stabilization by the medium (solvent type, ionic strength, and surfactant concentration) in agreement with the “aggregative growth” mechanism, rather than by solely the hydrolysis and condensation rates conventionally used for data interpretation in the classical nucleation theory. Medium properties (pH, ion types and concentration, polarity) also defined the efficiency of silica-surfactant cooperative self-assembly, which directly affected the porosity, mesopore size and pore wall thickness. Interestingly, this traditional silica-surfactant route showed a limited effect on the particle size, emphasizing the dominating role of colloidal stabilization in the studied reaction conditions. In situ pH measurements showed that every reaction medium has unique pH evolution profiles depending on the buffer capacity, hydrolysis and condensation rates. Reaction systems that fail to maintain the working pH can lead to non-porous products or undesired particle morphology and size distribution. The established particle formation mechanism allowed us to formulate comprehensive guidelines for preparing relatively concentrated colloids of near monodisperse (PDI 5-15%) mesoporous 30-700 nm silica spheres with variable porosity and mesopore size. These findings will be particularly useful in designing new mesoporous silica-containing materials for biomedical applications.

Keywords: mesoporous silica nanoparticles, MSN, colloidal stability, nucleation

■ INTRODUCTION

Over the last decade, mesoporous silica nanoparticles (MSN) have been attracting increasing attention as promising materials, in particular, because of their potential applications in drug delivery and biotechnology.¹⁻⁶ The mesoporous structure of the particles enables their loading with any material of choice – organic molecules, metal nanoparticles and quantum dots, luminophores, fluorophores, magnetic compounds – thereby endowing the particles with plasmonic, photoluminescent, fluorescent, and magnetic properties.^{5,7,8} Tunable particle size and porosity, monodispersity, easy framework modification, and reproducible analytical response made these materials a popular object of study in the emerging bioanalytical applications^{9,10} such as theranostics, immunodiagnosics, bioimaging, and bio- and chemosensors. For the same reasons, these materials also receive attention in catalysis and optoelectronics.⁷

Silica nanoparticles with mesopores in the range of 2-30 nm are commonly prepared by the condensation of silica precursors in the presence of

surfactant micelles and a catalyst in an aqueous medium.¹¹ The formation of the mesoporous framework proceeds via the cooperative self-assembly of the hydrolyzed silica precursor (silica alkoxides TEOS, TMOS,¹²⁻¹⁴ their functionalized derivatives⁵, sodium silicates¹⁵) onto the surfactant micelles.

In the early version of this mechanism, the main driving force was “charge density matching” that brings silica building blocks to the oppositely charged surface of surfactant micelles and facilitates subsequent silica condensation.¹⁶ Later, depending on the choice of the silica precursor and surfactant, self-assembly was found to be driven not only by electrostatic forces but also hydrogen bonding or weak Van der Waals interactions.¹¹ Cationic surfactants S⁺ (CTAB and derivatives) are usually chosen in the base-catalyzed systems with negatively charged silica clusters I⁻, and the self-assembly process could be simplistically described as S⁺I⁻ or S⁺X⁻M⁺I⁻ (where M⁺, X⁻ - counterions).⁷ For the non-ionic surfactants, acid-catalyzed systems with positively charged silica clusters (S⁰X⁺I⁺ or S⁰H⁺X⁺I⁺) are more often reported.¹⁷ There are also some examples of mesoporous silica formation in the

Table 1. The reagent molar ratio and reaction condition ranges used in the preparation of mesoporous silica particles.

Si	Molar ratios			EtOH vol. % in the solvent	Ionic strength of the solution, M	T, °C
	CTAB	TEA	Solvent			
1	0.02-0.21	0.001-2.3	80-500	0-30	0.0-0.2	0-80

presence of anionic surfactants S-I⁺, with amino-functionalized alkoxy silanes as a silica precursor.¹⁸

Hydrolysis and condensation of silica precursors can be effectively catalyzed by both H⁺ and OH⁻, which in practice leads to different product morphology.^{19,20} Since H⁺-catalysts favor the reactions with less electrophilic silica clusters (ideally, non-hydrolyzed TEOS), these systems generally produce too many linear oligomer nuclei* that uncontrollably aggregate or even form a gel-like product. However, even under these conditions, it is possible to obtain near monodisperse particles using very diluted solutions and/or a sufficient amount of stabilizer or surfactant.²¹⁻²⁴ OH-producing base catalysts, on the other hand, facilitate the reactions of more electrophilic silica clusters (ideally SiO_x(OH)_{4-x}), which is more convenient for producing sols – suspensions of colloiddally stable nanoparticles.

Therefore, to obtain near monodisperse colloiddally stable MSN, we mainly focused on the systems with the base as the hydrolyzing agent, CTAB as the cationic surfactant, and TEOS as the silica precursor. Such reaction systems were extensively studied over the last 30 years for the synthesis of *aggregated mesoporous solids* in terms of mesopore order, symmetry, size and shape, and framework stability.^{11,25}

However, very little systematic work has been done in application to the recently emerged *near monodisperse, colloiddally stable* 20-500 nm mesoporous (organo)silica nanoparticles for biomedical applications. The necessity to maintain sufficient colloiddal stabilization during the nanoparticle formation poses certain limitations on the synthetic conditions (higher dilution, lower reaction rates and ionic strength, avoiding hydrothermal treatment and calcination, and so on), which makes this area of research diverge even more from the typical practices in the preparation of mesoporous materials. A brief overview of the core literature on the preparation of MSN colloids can be found in the Supporting Information. It covers the role of the surfactant concentration²⁶⁻²⁹, the type and

amount of hydrolyzing agents^{12,13,23,30-37}, the effect of various kosmotropic and chaotropic salts^{11,25,38-50}, alcohol additives^{13,14,51-54}, and the degree of dilution^{13,31,36,55} in the nanoparticle formation mechanism. However, despite a large number of publications on the MSN synthesis and applications, the vast data on MSN preparation, undeniably valuable from the experimental point of view, is still poorly understood. Therefore, there is a need for a hypothesis resolving the contradictory trends observed for the systems with varied pH, surfactant, T, etc.

Traditional papers on mesoporous silica formation^{11,17,25} interpret their findings on the basis of cooperative self-assembly mechanisms that do not address the colloiddal aspects important for MSN particle formation. Some attempts have been made to explain the particle shape and size distribution in terms of the balance between the cooperative assembly energy and colloiddal stabilization energy.⁴⁶ However, the study investigated the traditional mesoporous silica synthesis and related to the crystal morphology rather than truly colloiddally stable MSN.

The reviews⁵⁶ and articles^{12,30} on colloiddally stable MSN often tend to explain the particle formation mechanism in terms of the Classical Nucleation Theory (LaMer model⁵⁷), which recently has been getting more critique⁵⁸⁻⁶⁰ in the nanoparticle synthesis community. Some researchers^{22,61} ascribed the observed deviations from the LaMer model to the interference from silica-surfactant self-assembly that affects particle nucleation. However, these aberrations seem to occur in many surfactant-free systems^{60,62} too, indicating that silica-surfactant assembly is not the key parameter in controlling the particle nucleation. More advanced non-classical models^{60,63-65} were developed to explain the nanoparticle formation mechanism via the “aggregative growth[†]” of the primary nuclei[‡], which takes both the reaction kinetics and colloiddal particle stabilization into consideration. The “aggregative growth” model successfully predicts the particle size trends in the synthesis of metal nanoparticles and

* In this paper, *nuclei* are used in its broad meaning as the products of a nucleation event. Nucleation in our systems is the formation of a new solid phase (silica clusters, oligomers, nanoparticles) from the monomer-saturated reaction medium.

† *Aggregative growth* – aggregation of various silica nuclei that produces larger nanoparticles. Unlike the uncontrollable aggregation, the process can result in the near monodisperse products if it has characteristics close to the ones in “fast nucleation”, namely: it involves all the present nuclei and occurs for a relatively short time.

‡ *Primary nuclei* are the early products of the first nucleation event – small partially hydrolyzed/condensed oligomeric silica clusters made of Si(OEt)_x(OH)_y(OSi)_z units.

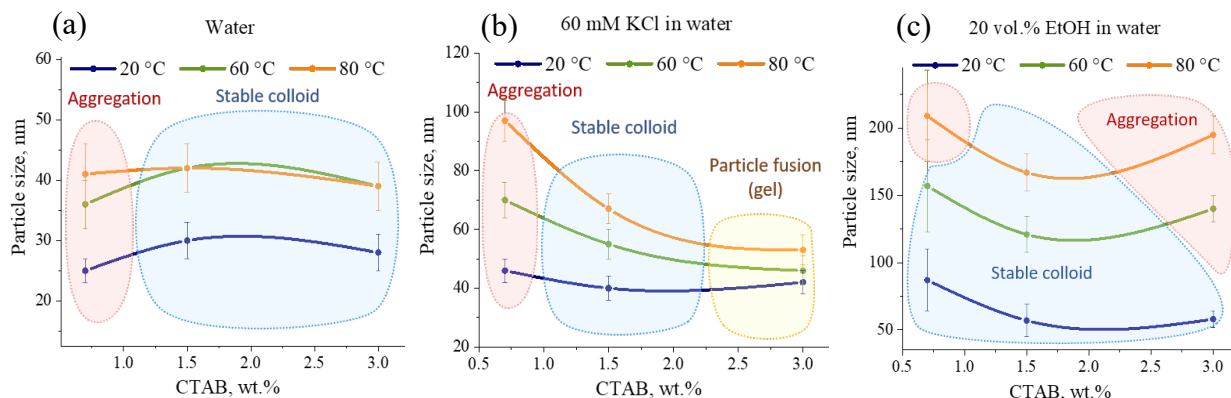


Figure 1. The reaction temperature and CTAB concentration effect on the particle size in different reaction media (Si:CTAB:TEA:Solvent=1:0.03-0.12:0.06:80).

non-porous Stöber silica spheres. There are reasons to believe that the surfactant-assisted sol-gel silica synthesis is not an exception.

Hence, the present work aimed to look beyond the traditional cooperative self-assembly mechanism and study the synthesis of mesoporous silica nanoparticles from the perspective of colloidal chemistry. Our experimental study allowed us to formulate the guidelines for preparing near monodisperse (PDI<15%) MSN with tunable size and mesoporous texture in basic conditions, which will help the researchers in pharmaceutical, biomedical and analytical areas. We have examined the role of pH, CTAB concentration, temperature, type of

hydrolyzing agent, ionic strength, and medium polarity in particle formation and found that the Bogush-Zukoski “aggregative growth” mechanism (which fundamentally includes but is not limited by the cooperative silica-surfactant assembly) is the best concept for explaining the vast diversity of the observed colloidal products.

■ EXPERIMENTAL SECTION

Materials. All the reagents were used in the synthesis as received without further purification: tetraethylorthosilicate (TEOS, 98%, Alfa Aesar), triethanolamine (TEA, free base, MP Biomedicals), ammonia solution (28-30 wt.%, EMD, GR ACS), cetyltrimethylammonium bromide (CTAB, >98%, Sigma), ethanol (anhydrous, Decon Labs), potassium fluoride, chloride, bromide and iodide, sodium chloride and iodide (AR, Mallinckrodt Chemicals), cesium chloride (99.9%, Aldrich), ammonium chloride (99.7%, Fischer Chemical), trimethylammonium and triethylammonium chloride (98+%, Acros Organics), tetrabutylammonium iodide and tetraoctylammonium chloride (98%, Sigma-Aldrich), potassium/sodium hydrophosphate and potassium dihydrophosphate (AR, Mallinckrodt Chemicals), pH buffers (Fisher Chemical), hydrochloric acid (concentrated, Fluka). Millipore® water (18 M Ω -cm) used in all

experiments was obtained from a Barnstead “E-pure” water purification system.

Instrumentation. The dynamic light scattering technique failed to provide adequate data for the wide range of the studied samples (including the aggregated systems) without special parameter adjustment, which is a common issue frequently brought up in the literature⁶⁶. For consistency, the morphology and shape of the particles were studied by TEM using the JEOL 1400 microscope with an acceleration voltage of 120 kV. Average particle size and standard deviation were calculated from measuring 150-250 particles using the ImageJ software. For monitoring particle size at different reaction times, the reaction mixture was diluted with cold ethanol 10 times, stored in a freezer, and analyzed by TEM without any preliminary washing. The textural properties were studied by low-temperature N₂ adsorption on the instrument Micromeritics ASAP 2020. The degassing procedure was carried out at 200 °C for 4 h under 1 μ m Hg vacuum, and the isotherm was recorded in the pressure range of P/P₀=0.002-0.99. The specific surface areas were calculated using the multipoint BET method at P/P₀=0.05-0.25, the pore size distributions – by BJH (cylindrical pores) on the adsorption branch of the isotherm (see SI for more details on the choice of model).

In situ pH measurements were carried out with the Mettler Toledo Seven Easy pH-meter with LabX-Direct software using a combination double-junction gel-filled glass membrane electrode with Ag/AgCl reference. Before each measurement, the pH meter was calibrated against standard buffer solutions (pH=4, 7, 10, 11) at the synthesis temperature of 60 °C. After each measurement, the electrode was thoroughly cleaned using an ultrasonic bath and rehydroxylated in 0.1 M HCl/1 M KCl solution for 1 h. The obtained pH curves were reproducible within an absolute error $|\Delta\text{pH}|$ of ~ 0.05 .

Preparation of Triethanolamine Hydrochloride (TEAHCl). Triethanolamine (10 mL) was dissolved in 10 ml of DI water and neutralized with 9.1 ml of concentrated hydrochloric acid (final pH ~ 6.5) under constant stirring at 0°C to prevent the mixture from overheating. The white crystalline powder was washed with 50 ml of ethanol three times and dried in an oven at 60°C overnight.

Preparation of mesoporous nanoparticles. A procedure for preparing mesoporous nanoparticles was developed based on a recipe producing reasonably concentrated ~ 4 wt.% colloids with a relatively low hydrolyzing agent and surfactant content³⁷. In a typical experiment, a flat-bottom glass flask with a certain amount of CTAB, TEA, and solvent was placed in an oil bath at 60 °C. The system was equilibrated for 20 min, and TEOS was added at once to the mixture. To reduce the effect of stirring on the particle formation, we used 20 ml vials with ~ 10 mm stirring bars to ensure rapid TEOS emulsification. After 15-20 h of vigorous mixing at the selected temperature, the resulting iridescent or white colloid was collected and washed twice with ethanol to remove the unreacted TEOS and four-six times with a hot 0.02 M HCl solution in ethanol to remove the surfactant from the mesopores. The typical reagent molar ratio was Si : CTAB : Hydrolyzing Agent : Solvent = 1 : 0.06 : 0.02-0.08 : 80, the reaction yields were $> 90\%$ for all the studied systems. The synthesis parameters were varied in the range presented in Table 1.

RESULTS

Temperature and surfactant content screening

In preparation for studying the effect of the hydrolysis rate and colloidal stabilization by medium, we screened a range of reaction temperatures and surfactant concentrations to define the conditions that lead to a near monodisperse product (PDI 5-15%) with good yields $> 90\%$ (~ 4 wt.% colloid).

The entire T range of 20-80 °C produced nanoparticles with reasonable yields ($>90\%$); however, the reaction rates at $T < 20$ °C were too slow and considered impractical due to the increased probability of forming emulsion-templated side-products (Figure SI1a and Figure SI2a). Varying the surfactant concentration showed that nanoparticles usually become prone to fusion/aggregation at the CTAB content below 0.7 wt.% at the later synthesis stages (Figure SI1b). Above 5 wt.% CTAB,

spontaneous micelle self-assembly might be induced, producing large mesoporous crystals as a side-product (Figure SI2b).

The effect of T and CTAB concentration on the particle size seem to depend on the medium strongly. It was small for purely aqueous reaction media with low ionic strength and sufficient steric stabilization⁶⁷ provided by TEA (20-40 mM), but quite notable for the media with ethanol or salt additives (Figure 1, Figure SI3). A brief analysis of the complex profiles in Figure 1 led us to conclude that the conditions providing the lowest reaction/precipitation rates (fewer nuclei at lower T) and a thick protective surfactant or solvation shell around the particles demonstrated the smallest response to the variation in the reaction parameters, the reasons of which we will discuss later in more detail.

pH evolution and product morphology

Many papers on MSN synthesis pay special attention to the effect of pH and the corresponding hydrolysis rates on particle size.^{12,30,56} The effect is often explained in terms of the classical nucleation (or LaMer) model, where higher hydrolysis rates are supposed to result in higher supersaturation and, therefore, a larger number of nucleation events, producing smaller nanoparticles.

As the first step of our investigation, we tried to follow the same pathway and study a series of reactions with 1÷40 mM solutions of a common hydrolyzing agent TEA, which corresponded to the initial pH_0 range of 8.2-9.2. The pH of the mixture was monitored throughout the reaction by *in situ* pH measurements using a glass electrode.

The drop in the reaction pH was found to correlate with the product morphology. Based on the pH evolution analysis (see SI for more details), we can speculate that for the sufficient TEA amount > 15 mM the pH did not decrease dramatically during the most

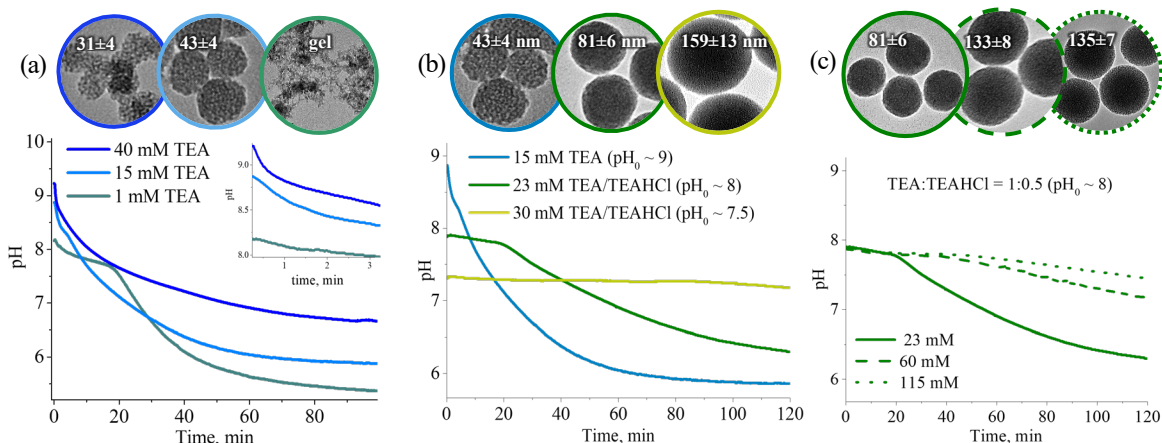


Figure 2. Evolution of the pH of the reaction medium in the systems with different concentrations of TEA or TEA/TEAHCl (molar ratios Si : CTAB : TEA : Solvent = 1 : 0.06 : 0.001-0.1 : 80, 60 °C). For more information about the systems with ammonia and phosphate buffers see Supplementary information (Figure SI5).

vital particle formation stages, which resulted in relatively near monodisperse colloidal particles with PDI < 15% (Figure 2a). For a lower TEA concentration < 1 mM, a significant pH drop happened during or even before nucleation, switching the reaction mechanism from base- to acid-catalyzed and leading to a mixed sol-gel or gel product (Figure 2a). Therefore, maintaining the working pH in the basic or subneutral range is expected to produce nanoparticle colloids.

Indeed, using the TEAHCl/TEA buffer with sufficient buffer capacity (23 mM, pH₀ ~ 8) enabled us to obtain a stable colloid of ~ 80 nm nanoparticles instead of a sol-gel mixture observed for 1 mM TEA at the same pH range (Figure 2b). Interestingly, the decrease in pH₀ from 9 to 7 was shown to notably increase the particle size from 30 to 160 nm, seemingly in accordance with the supersaturation concept predicting larger particles at lower hydrolysis rates. The same trend was observed for the ammonia and phosphate buffers, although the particle sizes differed for each buffer system (Figure S14).

However, we also observed the data points that didn't quite fit the Classical Nucleation Theory (CNT) model. For example, the increase in the buffer concentration notably increased the particle size for TEAHCl/TEA and phosphate buffer despite more basic working pH and, therefore, the higher hydrolysis rates (Figure 2c, Figure S14,5). Moreover, the reaction catalyzed by 20 mM of the phosphate buffer at pH₀=6 surprisingly produced a colloid of 80 nm nanoparticles instead of the expected gel.

All of the above made us conclude that the initial or working pH were not the main reaction parameters that controlled the particle formation mechanism. It seems that buffers have another characteristic not directly related to their H⁺/OH⁻ generation ability –

their contribution to the ionic strength and specific interactions with the growing silica clusters (Figure S16). These findings prompted us to undertake further investigation of the role of the ionic strength and the reaction medium stabilizing properties in the particle formation mechanism.

The effect of salt additives

To study the role of ionic strength in the particle formation mechanism, we screened a set of non-hydrolyzing salts M⁺X⁻ (M⁺ = Na⁺, K⁺, Cs⁺, TMA⁺, TEA⁺, TBA⁺, and X⁻ = F⁻, Cl⁻, Br⁻, I⁻) at different concentrations.

The addition of salts is expected to facilitate silica hydrolysis, condensation, and silica-surfactant mesophase formation due to the suppressed solvation shell.^{11,25,44-46} The lower pH drop along with higher precipitation rates observed in our systems in the presence of salts point to the higher condensation rates (Figure 4a, Figure S17 for more detailed discussion).

Regardless of the ion type, the higher ionic strength up to 0.1 M produced larger but still near monodisperse (PDI < 15%) mesoporous nanoparticles (Figure 3a). Fluoride salts were an exception due to their high catalytic activity^{19,68} in hydrolysis and condensation, producing multiple stabilized nuclei at the earliest reaction stages. The further increase in the ionic strength > 0.1 M resulted in particle fusion (Figure 3a insets), pointing to insufficient colloidal stabilization at the later synthesis stages. Moreover, the high ionic strength also shifted the reaction towards a sol formation in the systems that normally produce a gel (Figure S18). Similarly, the addition of 1 M KCl induced the cooperative silica-surfactant assembly into the ordered mesoporous structures in the system that only produces 20-30 nm nanoparticles with disordered porosity without salt (Figure S19).

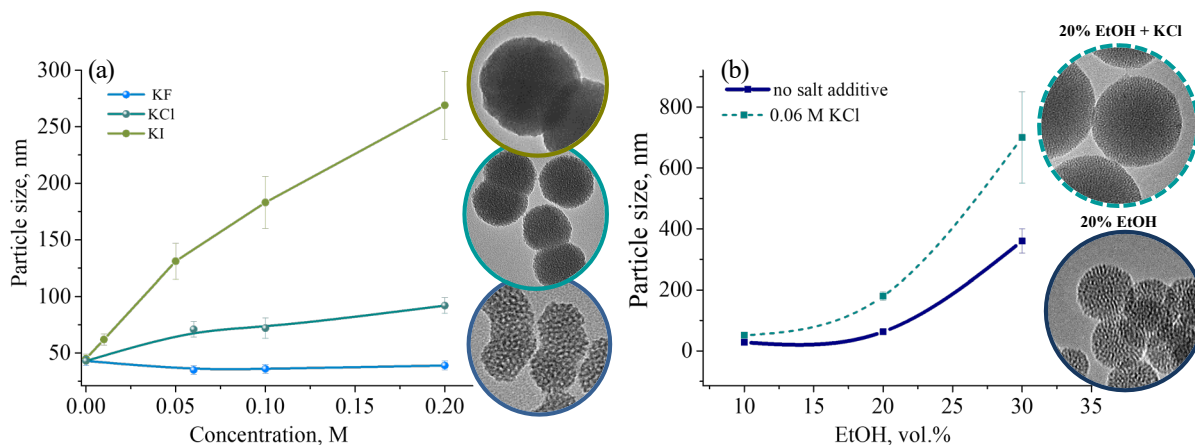


Figure 3. The effect of additives concentration on the particle size: (a) monovalent anions at 20 mM TEA (Si : CTAB : Solvent = 1 : 0.06 : 80, 60 °C); (b) ethanol content with and without salt additive (Si : CTAB : TEA : Solvent = 1 : 0.21 : 2.3 : 500, 60 °C).

Different ions seem to facilitate reaction rates and affect particle stabilization to a different extent. The particle diameter increased from the highly hydrated “hard” kosmotropic to the weakly hydrated “soft” chaotropic ions: $F^- < Cl^- < Br^- < I^-$ for potassium salts (Figure 4a). Screening various cations in a wide range from kosmotropic Na^+ to chaotropic Cs^+ or bulky TEA^+/TBA^+ showed a minor effect on the particle size (Figure SI10). The pH evolution profiles follow the observed particle size trends: the increase in the working pH from more hydrated Cl^- to chaotropic I^- and no significant changes for cations (Figure SI7).

Therefore, the larger and less hydrated *anions* increase the particle size to a greater extent, most likely due to the ability to better screen the particle surface charge and, thereby, induce their growth by the aggregation of silica clusters. Various types of *cations* did not demonstrate statistically significant differences suggesting that their influence is overwhelmed by the anions, which generally have a larger size and are believed to have more impact on colloidal systems.⁵⁰

Interestingly, the salt-induced particle size enlargement seems to be less significant if the loss of a thick hydration shell is partially compensated by other factors, for example, the high concentration of a steric stabilizer TEA or the ionic surfactant. From the colloidal point of view, the low reaction temperature can also improve particle stabilization by generating fewer building blocks and significantly reducing their collision frequency in the solution.⁶⁹ The screening of the reaction T (20-80 °C) and CTAB concentration (0.7-3.0 wt.%) in 60 mM KCl solution clearly demonstrated that the particle size enlargement was barely noticeable at the lowest T for all CTAB contents and the highest CTAB content for

all temperatures (Figure 1b). It suggests that the particle size is dominated by the colloidal stabilization or the surfactant protective shell, and the system shows a noticeable response to the changes in the reaction rates only when these factors are reduced.

The effect of EtOH additives on particle size

Similar to salts, adding ethanol increases the particle size from 50 to 500 nm (Figure 3b, Figure SI11). On the one hand, ethanol slows down the *apparent* reaction rate due to the reverse H^+/OH^- -catalyzed silica alcoholysis¹⁹, well-known for the base-catalyzed systems. Our experiments also confirmed slower precipitation rates along with the slower pH evolution (Figure 4a). In line with the supersaturation concept, the smaller monomer buildup should produce fewer nuclei that eventually reach a larger size.

On the other hand, above a 20 vol.% EtOH threshold, we observe fused nanoparticles, which points to the loss of the electrostatic stability in the medium with low dielectric permittivity. Just as in the case of salts, we can speculate that the medium’s decreased colloidal stabilization may facilitate the aggregation of silica-surfactant clusters producing fewer nuclei and larger nanoparticles.

Surprisingly, the variation of T and CTAB content for the 20 vol.% EtOH- H_2O mixture did not show the same trend as for 60 mM KCl. The larger CTAB content (3 wt.%) did not lead to the expected decrease in the particle size due to the surfactant protective layer. On the contrary, the dependence showed a curve with a local minimum at 1.5 wt.% CTAB, more pronounced at the higher temperatures (Figure 1c). It’s worth noting that the ability of CTAB to form micelles and stabilizing double layers

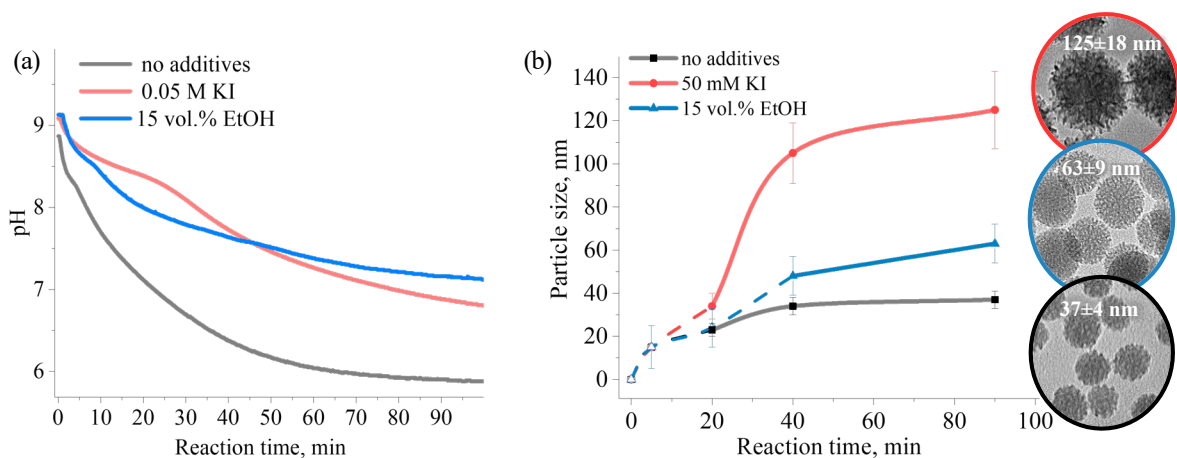


Figure 4. The effect of salt and ethanol additive on the pH evolution (a) and evolution of the particle size in the different reaction media monitored by TEM(b). Solid lines indicate the time intervals when nanoparticles were clearly observed; dashed lines – when only vague signs of particles/micelles/droplets were seen. (Si : CTAB : TEA : Solvent = 1 : 0.06 : 0.03 : 80, 60 °C).

Table 2. Textural properties of the prepared mesoporous silica nanoparticles.¹

Sample	$D_{TEM},^2$ nm	$S_{BET}, m^2/g$	$S_{meso},^3 m^2/g$	$V_{meso},^3 cm^3/g$	Sample	$D_{TEM},^2$ nm	$S_{BET}, m^2/g$	$S_{meso},^3 m^2/g$	$V_{meso},^3 cm^3/g$
TEA content					Anion type				
5 mM TEA	39±4	162	75	0.06	KF	30±3	706	648	0.46
15 mM TEA	38±4	602	521	0.27	KCl	50±4	642	609	0.41
40 mM TEA	42±4	612	532	0.37	KBr	56±5	670	636	0.41
50 mM TEA	31±4	709	637	0.43	KI ³	109±13	558	513	0.47
75 mM TEA	33±5	793	714	0.53	Cation type Cl ⁻				
20 mM $K_xH_{3-x}PO_4$ buffer					NaCl	53±5	711	678	0.44
pH=8	57±4	334	270	0.19	KCl	50±4	642	609	0.41
pH=7	61±5	114	70	0.06	CsCl	49±5	703	658	0.44
pH=6	70±5	97	30	0.03	TEACl	49±4	608	559	0.37
Ethanol content (at 40 mM TEA)					Cation type I ⁻				
10 vol.% EtOH	48±6	733	674	0.40	NaI	99±10	643	624	0.51
20 vol.% EtOH	104±10	644	592	0.33	KI	109±13	558	513	0.47
30 vol.% EtOH	442±28	199	156	0.08	TBAI	116±12	526	402	0.36

¹ The reaction ratio was Si : CTAB : Solvent = 1 : 0.06 : 80, 60 °C, the concentration of all the F⁻, Cl⁻ and Br⁻ salts was 60 mM at $C_{TEA}=40$ mM. The concentration of I⁻ salts was chosen to be 50 mM due to the lower CTAI solubility at the given temperature.

² The nanoparticle diameter was determined by analyzing 150-250 particles in TEM images.

³ To reduce the contribution of interparticle mesoporosity and intrinsic micropores, $V(S)_{meso}=V(S)_{total}-V(S)_{micro}-V(S)_{BJH(>10 \text{ or } 20 \text{ nm})}$, where $V(S)_{BJH(>10 \text{ or } 20 \text{ nm})}$ was estimated for the P/P₀ corresponding to the mesopores > 20 nm for I⁻-containing samples and > 10 nm for the rest samples using the BJH model. For more information see the SI.

decreases with higher T and alcohol content in the mixture.⁷⁰⁻⁷² In a certain medium, the excess of CTAB may not only lose its stabilizing properties but even induce small nuclei or even particle aggregation (Figure SI3) due to the so-called “depletion” or “hydrophobic” colloidal effect, which was reported for suspensions of non-porous silica nanoparticles.⁷³

Reaction kinetics or aggregation as the main factor for particle size enlargement?

According to the literature and the data discussed in the previous sections, salt and ethanol additives affect the apparent hydrolysis/condensation rates in opposite directions. Therefore, we would expect to see some mutual cancelation of their contributions in the mixed reaction medium. However, we observed even larger nanoparticles (Figure 4), and the synergy between the two effects grew as the ethanol content increased.

The only parameter that could be synergistically affected by salt and ethanol additives is the loss of electrostatic colloidal stabilization by the medium. To further investigate this matter, we monitored the particle formation in the presence of KI and EtOH throughout the synthesis using TEM (Figure 4, Figure SI12).

Comparative analysis of the TEM images at 20 min of the reaction confirmed the faster formation of nanoparticles in the presence of salt (30 nm vs. 20 nm for the reference) and slower precipitation of nanoparticles in the presence of alcohol (no signs of nanoparticles, Figure SI12). During the next 20 min, the particles dramatically grew up to 100 nm in the

KI sample and only slightly increased in the reference sample. Remarkably, the EtOH-containing system evolved from the state with no distinct structures to 50 nm nanoparticles and surpassed the reference sample over the same period, despite its overall reaction kinetics being relatively slow. These findings demonstrate that the lower colloidal stabilization in the alcohol- or salt-containing media can be more decisive in defining the final particle size than the hydrolysis rates. The effect of the stabilizing medium is briefly summarized in Figure 5.

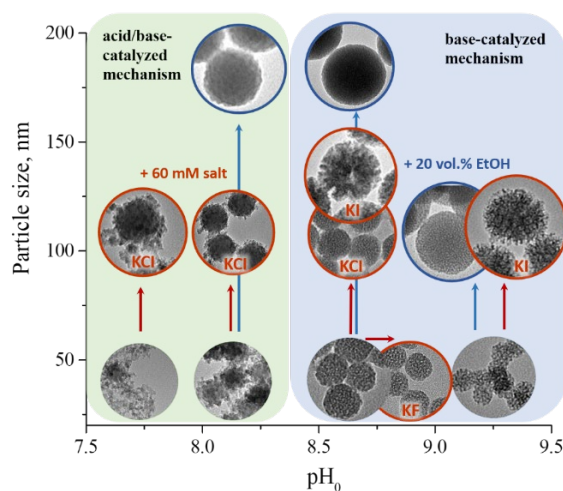


Figure 5. Variety of products obtained with different reaction media and with 1-100 mM TEA as a hydrolyzing agent (Si : CTAB : Solvent = 1 : 0.06 : 80, 60 °C). Note: salts or ethanol generally increase the particle size, with F⁻ being an exception due to its high intrinsic catalytic activity.

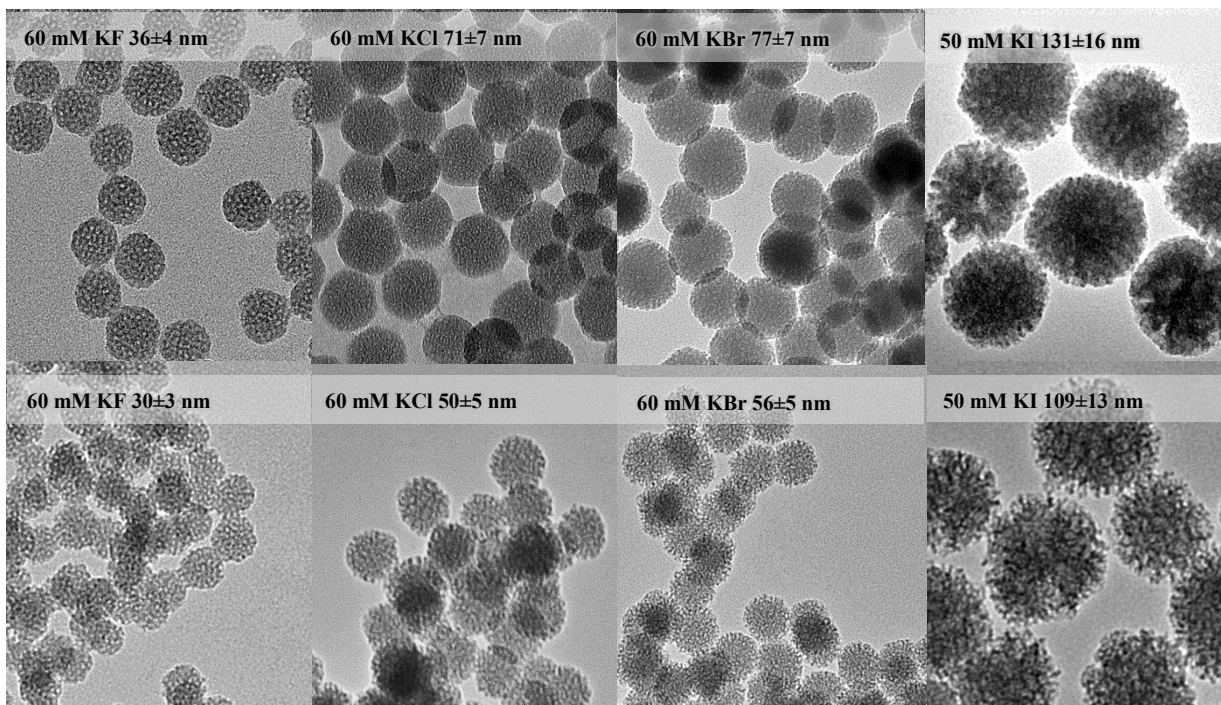


Figure 6. TEM images of the particles obtained with different potassium halides: at 15 mM TEA (top) and at 40 mM TEA (bottom). (Si : CTAB : Solvent = 1 : 0.06 : 80, 60 °C).

The crucial role of colloidal stabilization in particle synthesis is clearly illustrated by the formation of “raspberry-like” nanoparticles. This phenomenon takes place in the systems with the substantial pH drop that triggers “secondary” nucleation. Reducing the medium’s stabilizing properties can trigger the aggregation of the freshly formed nuclei onto the existing particles, giving rise to the raspberry-like morphologies. Interested readers can find more information about this mechanism in the Supporting Information (see “Bimodal particle size distribution and raspberry-like morphology,” Figures SI13-15).

Main factors affecting particle porosity

The mesopores in the studied materials result from the formation of a silica framework around the CTAB

micelles, and these interactions are believed to be driven by electrostatic forces between $\equiv\text{Si-O}^-$ and CTA^+ . Consequently, one can expect that medium properties would affect these interactions via the micelle packing parameter and effective surface charge, thereby resulting in different mesoporous structures.¹¹ Also, the degree and type of the particle mesoporosity will reflect the contribution of cooperative silica-surfactant self-assembly to the particle formation mechanism under different reaction conditions.

TEM images of the samples prepared with TEA, ammonia, and phosphate buffers indicate that the overall particle porosity decreases as the initial pH drops below 8 regardless of the choice of the hydrolyzing agent (Figure SI4-5). Textural properties

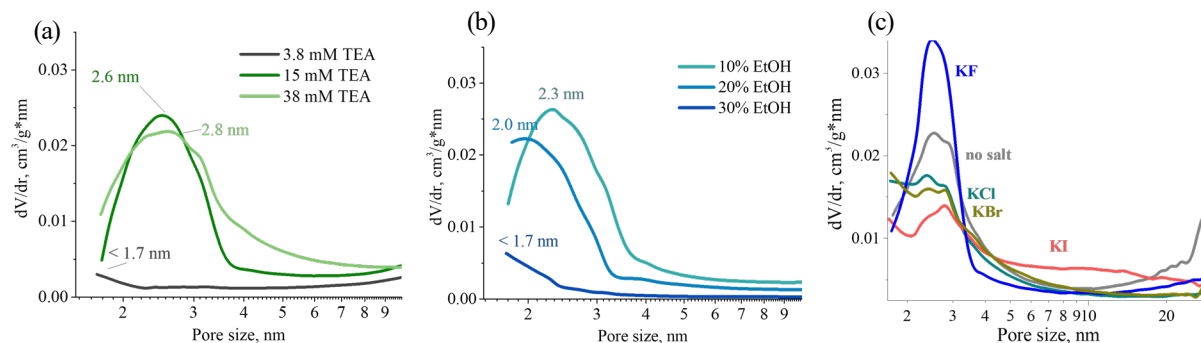


Figure 7. The effect of (a) pH (in H₂O), (b) medium properties (50 mM TEA) and (c) anion addition (60 mM salt and 50 mM TEA in H₂O) on the mesopore size distribution obtained by low-temperature N₂ adsorption (Si : CTAB : Solvent = 1 : 0.06 : 80, 60 °C).

obtained by low-temperature N₂ adsorption fully confirm that trend (Figure 6a, Table 2). On the one hand, lower pH decreases both ≡Si-OEt hydrolysis and ≡Si-OH dissociation and can suppress the silica-surfactant electrostatic interactions via the route CTA⁺O⁻-Si≡. Such systems favor silica condensation over silica-CTAB cooperative assembly during the nanoparticle formation, leading to the lower total mesopore volume and thicker silica walls.

The variation of the anion in the salt additive from highly hydrated kosmotropic F⁻ to chaotropic I⁻ also significantly changed the packing parameter of the micelles and, therefore, the mesoporous structure (Figure 7). The specific surface area and small mesopore volume slightly decrease from kosmotropic F⁻ to chaotropic I⁻, while the mesopore size increases and their distribution widens (Figure 6c, Table 2, Figure SI16-18). Although not so pronounced, the same dependence was observed for the cations Na⁺, K⁺, TEA⁺ and TBA⁺, with the CsCl and KBr samples slightly falling out of the trend for the unknown reason.

Interestingly, higher concentrations of kosmotropic salts and/or hydrolyzing agents seem to increase particle porosity (Figure SI5), most likely because of the higher working pH resulting from the facilitated condensation. Different anions seem to induce more pronounced textural changes at lower pH, where silanol dissociation and particle electrostatic stabilization are reduced (Figure 7, the upper and bottom row). The effect is likely to be explained by the competition between CTA⁺X⁻ and CTA⁺O⁻-Si≡, as we discuss later.

Ethanol addition slightly increases the mesopore volume at 10 vol.% due to the small micelle swelling effect observed for the low alcohol contents.⁷⁴ The higher ethanol concentration reduces the total mesopore volume even at relatively high pH₀ > 9, meaning that the concentration of ≡Si-O⁻ and CTA⁺ is insufficient for the effective S+I⁻ self-assembly in the medium with lower polarity (Figure 6b). The mesopore size also decreases at the higher ethanol content, which can be explained by the smaller CTAB micelle size due to their smaller aggregation number in the alcohol-containing medium.⁷⁰⁻⁷²

It is worth noting that the hydrophobic S⁰I⁰ interactions between the CTAB hydrophobic part and ≡Si-OEt also take place during the particle formation along with or instead of the electrostatic route, although such interactions do not yield highly porous products (V_{meso} ~ 0.1 cm³/g). DRIFT spectra of the washed low porosity samples showed an increased amount of CTAB compared to the highly mesoporous samples, and this surfactant residue was extremely hard to remove even by many repeated washes with

ethanolic HCl (Figure SI19). It points to the fact that silica nanoparticle formation proceeds via a spectrum of routes involving S+I⁻, S⁰I⁰ silica-surfactant interactions, and surfactant-free silica-silica condensation, each of them dominating under certain favorable conditions.

Practical advice for MSN design

Based on the extensive collected data, we have designed a set of general rules for the preparation of near monodisperse (PDI < 15%) particles with the desired size and mesoporous texture at subneutral-basic pH with CTAB surfactant (Figure 8):

1. The smallest nanoparticles < 50 nm form in the media with good electrostatic and/or steric stabilization – polar media with low ionic strength (< 0.05 M), TEA, reasonable surfactant excess, lower reaction T.

2. Larger spheres are produced in the media with diminished stabilization properties – less polar cosolvents (> 10 vol.% EtOH), high ionic strength (> 0.05 M), less CTAB, higher reaction T.

3. The variation in the reaction pH (which affects hydrolysis, condensation, and silica-surfactant assembly) can also be used to tune the particle nucleation/growth rates. However, the effect will be minimal for the media with good stabilizing properties.

4. The highly developed mesoporous pore system is usually formed in the reaction media where electrostatic interactions between silica and surfactant are favored – usually in sufficiently polar media at basic pH (> 8) in the presence of kosmotropic ions. Chaotropic ions result in lower porosity, larger mesopore size, and thicker pore walls.

5. The concentration and pK_a of the hydrolyzing agent affect the pH evolution profile. A large pH drop may induce the undesired aggregation, secondary nucleation or result in less porous particles, making it important to maintain pH above the critical level by using an appropriate buffer concentration. It is worth noting that a higher buffer concentration may also increase the ionic strength, contributing to particle size enlargement or aggregation in the absence of steric stabilization.

6. One should remember that ethanol reduces the reaction rates due to reverse alcoholysis reactions and generally decreases the porosity and mesopore size, which can be used for tuning the mesoporous structure to a certain extent. In order to stay within the reasonable range of reaction rates and porosities, one should limit its content to < 20 vol.%.

7. Salt additives, on the contrary, facilitate the reaction rates and accelerate the kinetics, which makes them a better tool for tuning the particle size. However, reaction media without stabilizing

additives and with the ionic strength > 0.05 M should be used with care because of their tendency to promote particle aggregation. The addition of 0.02-0.10 M kosmotropic (F^- , Cl^-) or chaotropic anions (Br^- , I^- , Tosylate) induces notable changes in the micelle aggregation number and S^+I^- electrostatic interactions, which makes it an easy and versatile tool for mesopore control comparable in the utility with organic porogens.²³ Swelling the micelles with cosolvents doesn't directly affect silica-surfactant interactions and usually results in highly porous structures with thin pore walls. Salt additives interfere with $S^+X^-M^+I^-$ interactions and allow us to vary not only the pore size but also the wall thickness, which can be useful for tuning particle degradability.

To illustrate the above guidelines, we provided a set of specific reaction conditions to prepare particles with various sizes, porosities, and a narrow particle size distribution (Figure SI20).

■ DISCUSSION

Mechanism of nanoparticle formation

Over the last 20 years, the research on mesoporous silica synthesis was mainly focused on the silica-surfactant interaction rather than the size and shape of the nanoparticles. A cooperative self-assembly mechanism was proposed, in which the silica-surfactant interactions enable the formation of the mesoporous silica framework and facilitate the precursor condensation.²⁵

However, new aspects of the mechanism have to be involved to predict the particle size distribution in these systems, namely: nucleation, growth, and colloidal stabilization. In terms of the particle nucleation, the self-assembly mechanism can be considered as a specific case of the sol-gel synthesis, where the nucleation stage is complicated by various silica-surfactant interactions (S^+I^- , $S^+X^-M^+I^-$, S^0X^0 , where S – surfactant, I – silica, M^+ , X^- – counterions) From this point of view, the surfactant is as much a part of the reaction medium as a solvent or stabilizer. In other words, the focus of the mechanism shifts from the “silica-surfactant” assembly to the more generalized “medium-mediated” silica assembly.

Such changes in the point of view will allow us to better explain the observed particle size trends in the MSN colloidal systems. However, which nucleation mechanism would fit the experimental data best? Many papers on nanoparticle synthesis^{12,30,56} tend to ascribe the seeming “pH-particle size” dependence (Figure SI6) and monodispersity to the classical nucleation mechanism⁷⁵ further developed by LaMer and Dinegar⁵⁷ by adding growth kinetics. In this model, the higher monomer buildup in the medium (=supersaturation) results in multiple nucleation events that eventually lead to the smaller nanoparticles. High monodispersity can be ensured by a very short nucleation stage where the entire population of nuclei forms in a nearly identical environment simultaneously.

All the above phenomena, without doubt, take place in every particle formation process. However, a

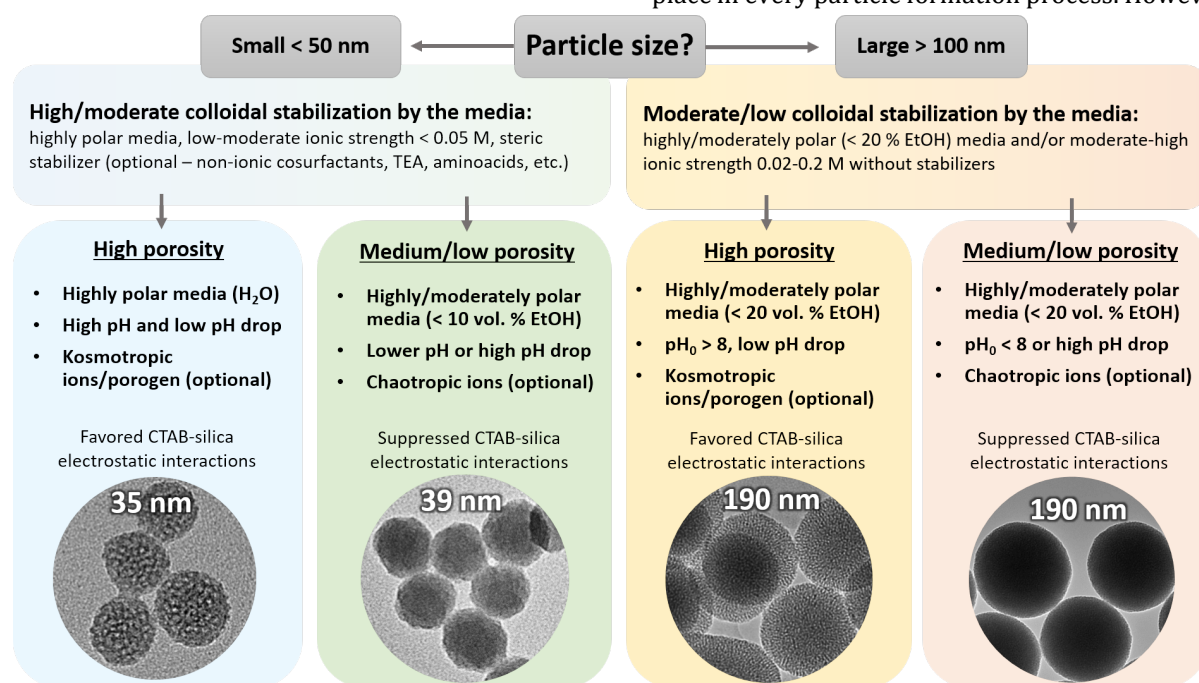


Figure 8. General rules to the formation of mesoporous silica nanoparticles with tunable size and porosity.

number of recent works claim that the classical nucleation theory doesn't define the *final* particle size distribution. In the early 1990s, G. H. Bogush and C. F. Zukoski⁶⁰ reported that the formation of well-known near monodisperse Stöber spherical particles seems to follow an "aggregative growth model," where particles grow by aggregation of generated silica clusters followed by monomer capture until they reach colloidal stabilization. However, this work didn't get as much attention as the classical nucleation mechanism in the nanoparticle synthesis literature. Later, the assumptions of the LaMer model were shown to be wrong not only for the originally studied sulfur⁵⁸, metal^{59,65}, and some inorganic oxide⁶⁵ colloids but also for the silica sol-gel synthesis¹³ where light scattering experiments showed that the number of particles increases throughout the synthesis instead of remaining constant.

In agreement with the "aggregative growth model" model, our *in situ* pH measurements and TEM observations for the systems with salt, ethanol, and stabilizer/surfactant additives suggest that the particles grow predominantly through the aggregation of silica clusters, and *their final size is mainly defined by the moment when they reach electrostatic or steric stabilization*. For example, we found that the higher salt concentration increases the reaction rate, whereas the higher ethanol content slows it down, yet both additives result in larger nanoparticles in all the studied pH range (Figure 5). Similarly, the systems seem to be not very sensitive to the moderate variation in pH (Table 2, TEA content), T, and CTAB concentration (Figure 1) if the particles are stabilized by at least one of the following factors: a thick protective shell from the excess of TEA, CTAB, a thick hydration shell from the low ionic strength and high medium polarity, smaller lower synthesis temperature (less frequent collision of building blocks). The systems with reduced colloidal stabilization (high ionic strength, low solvent polarity, low CTAB content, high T), on the contrary, readily respond to the changes in the reaction parameters (Figure 1b-c, Figure S13).

What makes nuclei aggregate

Let's look closer into the underlying phenomena driving nanoparticle colloidal stabilization or aggregation in the medium with different pH, ion content, and dielectric constant. First of all, the forming silica nanoparticles and clusters are covered with $\equiv\text{Si-OEt}$ and $\equiv\text{Si-OH}$ groups. The latter often dissociate in the reaction environment, with $\text{pK}_a \sim 2\text{-}9$ depending on the hydrolysis/condensation degree in $\text{Si}(\text{OH})_x(\text{OEt})_y(\text{OSi})_z$ building blocks and the working pH.^{38,76,77} According to the DLVO theory⁵⁹,

such nuclei or particles are better stabilized in the medium that:

- reduces the frequency of particle collision (low concentration or temperature);
- provides a thicker shell protecting the particles or silanols from interaction;
- increases the surface charge, in our case, by facilitating $\equiv\text{Si-OH}$ dissociation due to the charge stabilization by dipoles (like in a high dielectric constant solvent water at high enough pH).

A protective shell can be enriched with the solvent, stabilizer, surfactant molecules (like TEA, a single/double CTAB layer), cations and anions. For a hydrophilic surface, the lower ionic strength and more hydrated kosmotropic ions³⁸ usually reduce the surface charge screening, making the interparticle or silanol interactions more repulsive. For a predominantly hydrophobic surface, the colloidal stabilization is ensured by the steric stabilizer or surfactant molecules and chaotropic ions. All these factors become even more important for the early primary nuclei with high curvature that are even more prone to aggregation.⁵⁹

Let us consider the role of pH evolution in nuclei stabilization or aggregation. It is complicated by the fact that each reaction kinetics has a unique pH profile. The H^+ concentration usually increases due to the dissociation of the generated silanols and decreases due to the silanols condensation *and* the proton capture by the base. Too large and early pH drop may change the colloidal environment drastically, which may trigger secondary nucleation (Figure S13-15). Therefore, it is essential to maintain the pH above a critical level with an appropriate amount of buffer.

In addition to the higher buffer capacity, higher ionic strength and EtOH content were also found to increase the working pH, although it adds little to the overall electrostatic stabilization in these cases.

For example, both the particle size and working pH increases from more hydrated Cl^- to chaotropic I^- , which contradicts the literature reports on the Hofmeister series in hydrolysis/condensation.^{25,40} To resolve this contradiction, we propose that the particle growth is driven not only by the condensation reaction but also *the aggregation of nuclei* that are less electrostatically stabilized (or more screened) in the presence of chaotropic I^- .⁴¹ The forced nuclei aggregation "buries" the unreacted $\equiv\text{Si-OEt}$ and increases the chances of the available silanols condensation, which results in a smaller pH drop. This type of particle growth is not *directly* related to the condensation reaction but rather depends on the medium stabilizing properties.

The same aggregation-dominated process is likely to happen in alcohol-containing systems. Both the reduced hydrolysis rates and the decreased medium polarity result in primary nuclei with fewer charged groups, forcing them to aggregate even at the higher working pH. This might explain why the core of such nanoparticles has a relatively loose, not fully condensed framework full of unhydrolyzed $\equiv\text{Si-OEt}$.^{20,78} It is an important feature that makes it possible to produce hollow spheres from Stöber nanoparticles by selective etching and opens new approaches to nanoparticle design.⁷⁹

Reaction medium and particle porosity

The study of the mesoporous texture tells us that the presence of CTAB in the reaction medium does not necessarily induce S^+I^- interactions ($V_{\text{meso}}=0.08\div 0.53\text{ cm}^3/\text{g}$ for 5-75 mM TEA) or contributes to the facilitated particle growth (Table 2). It is the reaction medium that *enables electrostatic silica-surfactant interactions* determining the degree of particle mesoporosity. For base-catalyzed systems with a cationic surfactant, these interactions can be written in the form of S^+I^- or $\text{S}^+\text{X}^-\text{M}^+\text{I}^-$ (where S – surfactant, I – silica, MX – salt). Under this hypothesis, the factors reducing the net charge of the building blocks should result in the lower total porosity, as was fully confirmed in our experiments (Table 2). For CTA^+ micelles, these factors were high screening by ions, especially large chaotropic anions, and the suppression of ionic dissociation in the alcohol-containing medium. The charge of silica clusters was mostly reduced at subneutral pH and high EtOH content, as well as by high ion screening, especially with alkylammonium cations.

The *mesopore shape and size* follow the structure of the surfactant micelles, which, in turn, depends on the medium polarity, ionic strength, and solubilization of hydrophobic molecules. In accordance with this hypothesis, high ethanol content was shown to decrease the aggregation number of CTAB micelles due to the increased solubility of the hydrophobic “tail” eventually resulting in a smaller mesopore size. Similarly, the kosmotropic and chaotropic anions changed the hydrophilicity of the surfactant “head,” tuning the mesopore size from 2 for Cl^- to 10-20 nm for I^- .

Interestingly, ions seem to induce more pronounced changes in the systems at lower pH (Figure 7, the upper and bottom rows), as previously reported^{7,37} for chaotropic tosylate anions. According to the reported hypothesis, the dissociated silanols and anions compete for the adsorption onto the positively charged micelles, and it defines the porosity of the particles. The lower working pH (less $\equiv\text{Si-O}^-$) or more chaotropic anions (stronger binding

to CTAB) shift this competition in favor of the anions, which leads to low porosity products with larger mesopores. Thus, the formation of the highly developed mesoporous system depends on:

- the concentration of $\equiv\text{Si-O}^-$ that interact with positively charged micelles and trigger the cooperative self-assembly;
- the specific ion-mediated $\text{S}^+\text{X}^-\text{M}^+\text{I}^-$ interactions (where S – surfactant, I – silica, MX – salt).

On the order of the mesopores

Most MSN are prepared with stabilizers under “mild” hydrolysis conditions ($\text{pH}<10$) and possess “worm-like” disordered mesoporosity²³ (Figure 7, FigureS15), unlike classical ordered MCM-41 or MCM-48 materials. The reason for such a difference most likely lies in the precursor hydrolysis degree. The traditional ordered mesoporous silica syntheses^{13,31,36,55} provide the highest concentrations of $\equiv\text{Si-O}^-$ and CTA^+ at *high ionic strength* (FigureS19), resulting in fast precipitation within the first minutes of the reaction. Unfortunately, very high hydrolysis and condensation rates along with the high ionic strength do not allow the formation of colloidal stable MSN since the aggregative growth is too intensive and leads to large crystals or aggregated products. Moreover, the addition of a stabilizer would interfere with the self-assembly process, leaving the impractical “high dilution” approach as the only option for producing ordered near monodisperse MSN that are “protected” from aggregation by their low concentration ($\text{Si}/\text{solvent} < 1/600$).

However, some progress in improving the pore alignment can be achieved by manipulating the hydrophobic part of the micelles, for example – by using organic pore expanders. That topic is extensively covered in the recent review.⁷ The particles with stellar-like mesopores can be prepared by this approach in reasonable concentration without significant damage to the MSN colloidal stability.^{80,81}

■ CONCLUSIONS

In the present work, we have comprehensively studied the formation of near monodisperse ($\text{PDI} \sim 5\text{-}15\%$) 30-700 nm mesoporous nanoparticles in the subneutral-basic pH region of 6-11 using various hydrolyzing agents (triethanolamine, ammonia, phosphate buffers), CTAB concentration (0.5-5 wt.%) and reaction temperature (0-80 °C). The medium polarity was varied using ethanol additives (0-30 vol.%), and the ionic strength was tuned in the range of 0.001-0.2 M with monovalent salts M^+X^- , where $\text{M}^+ = \text{Na}^+, \text{K}^+, \text{Cs}^+, \text{TMA}^+, \text{TEA}^+, \text{TBA}^+$ and $\text{X}^- = \text{F}^-, \text{Cl}^-, \text{Br}^-, \text{I}^-$.

Screening of a wide range of reaction conditions showed that the cooperative assembly mechanism of mesoporous silica formation has limited applicability to the studied colloidal systems where silica-surfactant electrostatic interactions can be not a dominant route of the particle formation. The classic nucleation theory, where the particle size depends on nucleation rates tied to hydrolysis and condensation, also fails to explain the observed trends. We have found that the final particle size is defined by the medium's electrostatic or steric stabilization abilities, which confirms the Bogush-Zukoski model of aggregative growth. Under this hypothesis, the particle size becomes more sensitive to the changes in the reaction kinetics as colloidal stabilization decreases. The prerequisites for low colloidal stabilization are higher ionic strength or EtOH content, less surfactant or TEA stabilizer, usually more chaotropic anions, higher reaction temperature, lower pH.

These findings enabled us to formulate general rules for preparing near monodisperse mesoporous silica nanoparticles at a reasonable yield in a one-pot synthesis. We hope that these guidelines, along with understanding the mechanism of particle formation, will help the researchers develop new types of porous silica-containing nanoparticles. The present work can serve as a starting point for studying the formation of mesoporous silica nanoparticles with organic functional groups, where the interaction between silanols, surfactant, and organic moieties are even more complicated.

■ AUTHOR INFORMATION

Corresponding Author

viktroriyacatalysis@gmail.com

i.zharov@utah.edu

Notes

The authors declare no competing financial interest.

■ ACKNOWLEDGMENT

The work was fully supported by an Energy Frontier Research Center EFRC-MUSE funded by the US Department of Energy, Office of Science, Basic Energy Sciences, Award #DE-SC0019285.

■ REFERENCES

1. Vallet-Regí, M. Mesoporous Silica Nanoparticles: Their Projection in Nanomedicine. *ISRN Mater. Sci.* **2012**, 1–20 (2012).
2. Narayan, R., Nayak, U. Y., Raichur, A. M. & Garg, S. Mesoporous silica nanoparticles: A comprehensive review on synthesis and recent advances. *Pharmaceutics* **10**, 1–49 (2018).
3. Mehmood, A., Ghafar, H., Yaqoob, S., Gohar, U. F. & Ahmad, B. Mesoporous Silica Nanoparticles: A Review. *J. Dev. Drugs* **06**, (2017).
4. Linares, N. *et al.* Incorporation of chemical functionalities in the framework of mesoporous silica. *Chem. Commun.* **47**, 9024–9035 (2011).
5. Croissant, J. G., Fatieiev, Y., Almalik, A. & Khashab, N. M. Mesoporous Silica and Organosilica Nanoparticles: Physical Chemistry, Biosafety, Delivery Strategies, and Biomedical Applications. *Adv. Healthc. Mater.* **7**, 1–75 (2018).
6. Alahmadi S. Modification of Mesoporous Silica MCM-41 and its Applications- A review. *Orient. J. Chem.* **28**, 1–11 (2012).
7. Hao, P., Peng, B., Shan, B. Q., Yang, T. Q. & Zhang, K. Comprehensive understanding of the synthesis and formation mechanism of dendritic mesoporous silica nanospheres. *Nanoscale Adv.* **2**, 1792–1810 (2020).
8. Jafari, S. *et al.* Mesoporous silica nanoparticles for therapeutic/diagnostic applications. *Biomed. Pharmacother.* **109**, 1100–1111 (2019).
9. Gubala, V., Giovannini, G., Kunc, F., Monopoli, M. P. & Moore, C. J. *Dye-doped silica nanoparticles: Synthesis, surface chemistry and bioapplications. Cancer Nanotechnology* vol. 11 (Springer Vienna, 2020).
10. Jafari, S. *et al.* Mesoporous silica nanoparticles for therapeutic/diagnostic applications. *Biomed. Pharmacother.* **109**, 1100–1111 (2019).
11. Wan, Y. & Zhao, D. On the controllable soft-templating approach to mesoporous silicates. *Chem. Rev.* **107**, 2821–2860 (2007).
12. Qiao, Z. A., Zhang, L., Guo, M., Liu, Y. & Huo, Q. Synthesis of mesoporous silica nanoparticles via controlled hydrolysis and condensation of silicon alkoxide. *Chem. Mater.* **21**, 3823–3829 (2009).
13. Yano, K. & Fukushima, Y. Synthesis of mono-dispersed mesoporous silica spheres with highly ordered hexagonal regularity using conventional alkyltrimethylammonium halide as a surfactant. *J. Mater. Chem.* **14**, 1579–1584 (2004).
14. Yamada, H., Urata, C., Ujiie, H., Yamauchi, Y. & Kuroda, K. Preparation of aqueous colloidal mesostructured and mesoporous silica

- nanoparticles with controlled particle size in a very wide range from 20 nm to 700 nm. *Nanoscale* **5**, 6145–6153 (2013).
15. Lin, H. P. & Tsai, C. P. Synthesis of Mesoporous Silica Nanoparticles from a Low-concentration CnTMAX-Sodium Silicate Components. *Chem. Lett.* **32**, 1092–1093 (2003).
 16. Huo, Q. *et al.* Generalized synthesis of periodic surfactant/inorganic composite materials. *Nature* **368**, 317–321 (1994).
 17. Alothman, Z. A. A review: Fundamental aspects of silicate mesoporous materials. *Materials (Basel)*. **5**, 2874–2902 (2012).
 18. Han, L. & Che, S. Anionic surfactant templated mesoporous silicas (AMSs). *Chem. Soc. Rev.* **42**, 3740–3752 (2013).
 19. Brinker, C. J. Hydrolysis and condensation of silicates: effects on structure. *J. Non. Cryst. Solids* **100**, 31–50 (1988).
 20. Brinker, C. J. & Scherer, G. W. *Sol-Gel Science: The Physics and Chemistry of Sol-Gel Processing*. Academic Press Limited (1990). doi:10.1016/C2009-0-22386-5.
 21. Suzuki, K., Ikari, K. & Imai, H. Synthesis of Silica Nanoparticles Having a Well-Ordered Mesostructure Using a Double Surfactant System. *J. Am. Chem. Soc.* **126**, 462–463 (2004).
 22. Berggren, A. & Palmqvist, A. E. C. Particle size control of colloidal suspensions of mesostructured silica. *J. Phys. Chem. C* **112**, 732–737 (2008).
 23. Möller, K. & Bein, T. Talented mesoporous silica nanoparticles. *Chem. Mater.* **29**, 371–388 (2017).
 24. Gao, F., Botella, P., Corma, A., Blesa, J. & Dong, L. monodispersed mesoporous silica nanoparticles with very large pores for enhanced adsorption and release of DNA. *J. Phys. Chem. B* **113**, 1796–1804 (2009).
 25. Lin, H. P. & Mou, C. Y. Structural and morphological control of cationic surfactant-templated mesoporous silica. *Acc. Chem. Res.* **35**, 927–935 (2002).
 26. Vazquez, N. I., Gonzalez, Z., Ferrari, B. & Castro, Y. Synthesis of mesoporous silica nanoparticles by sol-gel as nanocontainer for future drug delivery applications. *Bol. la Soc. Esp. Ceram. y Vidr.* **56**, 139–145 (2017).
 27. Lelong, G. *et al.* Effect of surfactant concentration on the morphology and texture of MCM-41 materials. *J. Phys. Chem. C* **112**, 10674–10680 (2008).
 28. Chen, B. *et al.* In vitro and in vivo evaluation of ordered mesoporous silica as a novel adsorbent in liquid formulation. *Int. J. Nanomedicine* **7**, 199–209 (2012).
 29. Kim, M. K. *et al.* Optimization of mesoporous silica nanoparticles through statistical design of experiment and the application for the anticancer drug. *Pharmaceutics* **13**, (2021).
 30. Li, X. *et al.* A general method to synthesize a family of mesoporous silica nanoparticles less than 100 nm and their applications in anti-reflective/fogging coating. *J. Mater. Sci.* **51**, 6192–6206 (2016).
 31. Cai, Q. *et al.* Dilute solution routes to various controllable morphologies of MCM-41 silica with a basic medium. *Chem. Mater.* **13**, 258–263 (2001).
 32. Lai, C. Y. *et al.* A mesoporous silica nanosphere-based carrier system with chemically removable CdS nanoparticle caps for stimuli-responsive controlled release of neurotransmitters and drug molecules. *J. Am. Chem. Soc.* **125**, 4451–4459 (2003).
 33. Liu, J., Li, C. & Li, F. Fluorescence turn-on chemodosimeter-functionalized mesoporous silica nanoparticles and their application in cell imaging. *J. Mater. Chem.* **21**, 7175–7181 (2011).
 34. Lu, F., Wu, S. H., Hung, Y. & Mou, C. Y. Size effect on cell uptake in well-suspended, uniform mesoporous silica nanoparticles. *Small* **5**, 1408–1413 (2009).
 35. Lin, Y. S. *et al.* Well-ordered mesoporous silica nanoparticles as cell markers. *Chem. Mater.* **17**, 4570–4573 (2005).
 36. Yokoi, T., Karouji, T., Ohta, S., Kondo, J. N. & Tatsumi, T. Synthesis of mesoporous silica nanospheres promoted by basic amino acids and their catalytic application. *Chem. Mater.* **22**, 3900–3908 (2010).
 37. Zhang, K. *et al.* Facile large-scale synthesis of monodisperse mesoporous silica nanospheres with tunable pore structure. *J. Am. Chem. Soc.* **135**, 2427–2430 (2013).
 38. Sögaard, C., Funehag, J. & Abbas, Z. Silica sol as grouting material: a physio-chemical analysis. *Nano Converg.* **5**, 1–15 (2018).
 39. Xiang, W. D. *et al.* Synthesis of mesoporous silica by cationic surfactant templating in various inorganic acid sources. *Mater. Sci. Pol.* **28**, 709–730 (2010).
 40. Bagshaw, S. A. The effect of dilute electrolytes on the formation of non-ionically templated [Si]-MSU-X mesoporous silica molecular sieves. *J. Mater. Chem.* **11**, 831–840 (2001).

41. Lin, H. P., Kao, C. P., Mou, C. Y. & Liu, S. Bin. Counterion effect in acid synthesis of mesoporous silica materials. *J. Phys. Chem. B* **104**, 7885–7894 (2000).
42. Li, Y., Wang, Y., Huang, G., Ma, X. & Gao, I. A Surprising Chaotropic Anion-Induced Supramolecular Self- Assembly of Ionic Polymeric Micelles. *Angew Chem Int Ed Engl* **53**, 8074–8078 (2014).
43. Yu, C., Fan, J., Tian, B., Zhao, D. & Stucky, G. D. High-Yield Synthesis of Periodic Mesoporous. *Adv. Mater.* **14**, 1742–1745 (2002).
44. Issa, A. A. & Luyt, A. S. Kinetics of alkoxysilanes and organoalkoxysilanes polymerization: A review. *Polymers (Basel)*. **11**, (2019).
45. Yu, C., Tian, B., Fan, J., Stucky, G. D. & Zhao, D. Salt effect in the synthesis of mesoporous silica templated by non-ionic block copolymers. *Chem. Commun.* **24**, 2726–2727 (2001).
46. Yu, C., Fan, J., Tian, B. & Zhao, D. Morphology Development of Mesoporous Materials: A Colloidal Phase Separation Mechanism. *Chem. Mater.* **16**, 889–898 (2004).
47. Trompette, J. L. Influence of Co-Ion Nature on the Gelation Kinetics of Colloidal Silica Suspensions. *J. Phys. Chem. B* **121**, 5654–5659 (2017).
48. Van Der Linden, M. *et al.* Microscopic Origin of the Hofmeister Effect in Gelation Kinetics of Colloidal Silica. *J. Phys. Chem. Lett.* **6**, 2881–2887 (2015).
49. Tadros, T. F. & Lyklema, J. Adsorption of potential-determining ions at the silica-aqueous electrolyte interface and the role of some cations. *J. Electroanal. Chem. Interfacial Electrochem.* **17**, 267–275 (1968).
50. Gibb, B. C. Hofmeister’s curse. *Nat. Chem.* **11**, 963–965 (2019).
51. Matsoukas, T. & Gulari, E. Dynamics of growth of silica particles from ammonia-catalyzed hydrolysis of tetra-ethyl-orthosilicate. *J. Colloid Interface Sci.* **124**, 252–261 (1988).
52. Zainal, N. A., Shukor, S. R. A., Wab, H. A. A. & Razak, K. A. Study on the effect of synthesis parameters of silica nanoparticles entrapped with rifampicin. *Chem. Eng. Trans.* **32**, 2245–2250 (2013).
53. Issa, A. A., El-Azazy, M. & Luyt, A. S. Kinetics of alkoxysilanes hydrolysis: An empirical approach. *Sci. Rep.* **9**, 1–15 (2019).
54. Yamada, Y. & Yano, K. Synthesis of monodispersed super-microporous/mesoporous silica spheres with diameters in the low submicron range. *Microporous Mesoporous Mater.* **93**, 190–198 (2006).
55. Gu, J. *et al.* Sub-150nm mesoporous silica nanoparticles with tunable pore sizes and well-ordered mesostructure for protein encapsulation. *J. Colloid Interface Sci.* **407**, 236–242 (2013).
56. Wu, S. H. & Lin, H. P. Synthesis of mesoporous silica nanoparticles. *Chem. Soc. Rev.* **42**, 3862–3875 (2013).
57. LaMer, V. K. & Dinegar, R. H. Theory, Production and Mechanism of Formation of monodispersed Hydrosols. *J. Am. Chem. Soc.* **72**, 4847–4854 (1950).
58. Whitehead, C. B., Özkaz, S. & Finke, R. G. LaMer’s 1950 Model for Particle Formation of Instantaneous Nucleation and Diffusion-Controlled Growth: A Historical Look at the Model’s Origins, Assumptions, Equations, and Underlying Sulfur Sol Formation Kinetics Data. *Chem. Mater.* **31**, 7116–7132 (2019).
59. Polte, J. Fundamental growth principles of colloidal metal nanoparticles - a new perspective. *CrystEngComm* **17**, 6809–6830 (2015).
60. Bogush, G. H. & Zukoski, C. F. Uniform Silica Particle Precipitation: An Aggregative Growth Model. *J. Colloid Interface Sci.* **142**, 19–34 (1990).
61. Lv, X., Zhang, L., Xing, F. & Lin, H. Controlled synthesis of monodispersed mesoporous silica nanoparticles: Particle size tuning and formation mechanism investigation. *Microporous Mesoporous Mater.* **225**, 238–244 (2016).
62. Ghimire, P. P. & Jaroniec, M. Renaissance of Stöber method for synthesis of colloidal particles: New developments and opportunities. *J. Colloid Interface Sci.* **584**, 838–865 (2021).
63. Wang, F., Richards, V. N., Shields, S. P. & Buhro, W. E. Kinetics and mechanisms of aggregative nanocrystal growth. *Chem. Mater.* **26**, 5–21 (2014).
64. Cheng, H. W., Luo, J. & Zhong, C. J. An aggregative growth process for controlling size, shape and composition of metal, alloy and core-shell nanoparticles toward desired bioapplications. *J. Mater. Chem. B* **2**, 6904–6916 (2014).
65. Whitehead, C. B. & Finke, R. G. Particle

- formation mechanisms supported by in situ synchrotron XAFS and SAXS studies: a review of metal, metal-oxide, semiconductor and selected other nanoparticle formation reactions. *Mater. Adv.* **2**, 6532–6568 (2021).
66. Kaasalainen, M. *et al.* Size, Stability, and Porosity of Mesoporous Nanoparticles Characterized with Light Scattering. *Nanoscale Res. Lett.* **12**, (2017).
 67. Möller, K., Kobler, J. & Bein, T. Colloidal suspensions of nanometer-sized mesoporous silica. *Adv. Funct. Mater.* **17**, 605–612 (2007).
 68. Coltrain, B. K. & Kelts, L. W. The Chemistry of Hydrolysis and Condensation of Silica Sol-Gel Precursors. in *The Colloid Chemistry of Silica*. *Bergna, H.* 405–416 (American Chemical Society, 1994). doi:10.1088/1751-8113/44/8/085201.
 69. Huang, J. *et al.* Systematic approach to develop a colloidal silica-based gel system for water shut-off. *SPE Middle East Oil Gas Show Conf. MEOS, Proc.* **2017-March**, 2742–2756 (2017).
 70. Li, W., Zhang, M., Zhang, J. & Han, Y. Self-assembly of cetyltrimethylammonium bromide in ethanol-water mixtures. *Front. Chem. China* **1**, 438–442 (2006).
 71. Shah, S. K. & Bhattarai, A. Interfacial and Micellization Behavior of Cetyltrimethylammonium Bromide (CTAB) in Water and Methanol-Water Mixture at 298.15 to 323.15 K. *J. Chem.* **2020**, (2020).
 72. Nazir, N., Ahanger, M. S. & Akbar, A. Micellization of cationic surfactant cetyltrimethylammonium bromide in mixed water-alcohol media. *J. Dispers. Sci. Technol.* **30**, 51–55 (2009).
 73. Liu, Y., Tourbin, M., Lachaize, S. & Guiraud, P. Silica nanoparticles separation from water: Aggregation by cetyltrimethylammonium bromide (CTAB). *Chemosphere* **92**, 681–687 (2013).
 74. Bielawska, M., Chodzińska, A., Jańczuk, B. & Zdziennicka, A. Determination of CTAB CMC in mixed water+short-chain alcohol solvent by surface tension, conductivity, density and viscosity measurements. *Colloids Surfaces A Physicochem. Eng. Asp.* **424**, 81–88 (2013).
 75. Karthika, S., Radhakrishnan, T. K. & Kalaichelvi, P. A Review of Classical and Non-classical Nucleation Theories. *Cryst. Growth Des.* **16**, 6663–6681 (2016).
 76. Belton, D. J., Deschaume, O. & Perry, C. C. An overview of the fundamentals of the chemistry of silica with relevance to biosilicification and technological advances. *FEBS J.* **279**, 1710–1720 (2012).
 77. Onizhuk, M. O., Panteleimonov, A. V., Kholin, Y. V. & Ivanov, V. V. Dissociation Constants of Silanol Groups of Silic Acids: Quantum Chemical Estimations. *J. Struct. Chem.* **59**, 261–271 (2018).
 78. Li, S., Wan, Q., Qin, Z., Fu, Y. & Gu, Y. Unraveling the Mystery of Stöber Silica's Microporosity. *Langmuir* **32**, 9180–9187 (2016).
 79. Tang, F., Li, L. & Chen, D. Mesoporous silica nanoparticles: Synthesis, biocompatibility and drug delivery. *Adv. Mater.* **24**, 1504–1534 (2012).
 80. Maity, A. & Polshettiwar, V. Scalable and sustainable synthesis of size-controlled monodisperse dendritic fibrous nanosilica quantified by e-factor. *ACS Appl. Nano Mater.* **1**, 3636–3643 (2018).
 81. Polshettiwar, V., Cha, D., Zhang, X. & Basset, J. M. High-surface-area silica nanospheres (KCC-1) with a fibrous morphology. *Angew. Chemie - Int. Ed.* **49**, 9652–9656 (2010).

TOC Graphic

Medium controlled aggregative growth as a key step in mesoporous silica nanoparticle formation

Viktoriya Semeykina* and Ilya Zharov*

Department of Chemistry, University of Utah, Salt Lake City, UT 84112

